

# Formulation and Evaluation of Controlled Release Cefixime Nanoparticles Prepared using *Basella alba* Leaf Mucilage and Chitosan as Matrix Formers

B. Harika<sup>1</sup>, S. Shanmuganathan<sup>\*1</sup>, K. Gowthamarajan<sup>2</sup>

<sup>1</sup>Department of Pharmaceutics, Faculty of Pharmacy,  
Sri Ramachandra University, Porur, Chennai-600116, Tamilnadu, India,

<sup>2</sup>Department of Pharmaceutics, JSS College of Pharmacy,  
Rocklands, Ootacamund-643001, Tamilnadu, India

## Abstract

### Aim:

The present exploration was aimed to develop and to evaluate a novel polymer based controlled release cefixime nanoparticles prepared using *Basella alba* leaf mucilage and chitosan as drug carrier to achieve an effective therapeutic concentration and to overcome the limitations associated with conventional dosage forms.

### Methods:

The polymeric cefixime nanoparticles were prepared by the modified coacervation method. The cefixime nanoparticles were evaluated for particle size, zeta potential, morphological studies, entrapment efficiency, *in-vitro* drug release studies and *in-vitro* antimicrobial efficiency studies.

### Results:

The prepared formulations showed average particle size range from 165.5±6.5 to 399.8±6.3 nm. The surface morphology studies revealed that the nanoparticles were spherical with smooth surface and entrapment efficiency was found to be 71.6±1.2 to 80.53±4.5%. Further, the *in-vitro* drug release showed a biphasic pattern with initial burst release followed by sustained release of drug up to 24h. The *in-vitro* antimicrobial efficiency of the formulation showed better zone of inhibition with minimum concentration compared to pure drug.

### Conclusion:

The developed polymeric cefixime nanoparticles support to tailor the drug release profile with better antimicrobial efficiency for improving the patient compliance followed by the declining the limitations associated with antibiotics.

**Keywords:** Antimicrobial efficiency, *Basella alba* leaf mucilage, Cefixime, Chitosan, Controlled drug release, Polymeric nanoparticle.

## INTRODUCTION

Typhoid fever is a life-threatening febrile illness caused by the bacterium *Salmonella enterica* serotype Typhi habitually acquired through the ingestion of food or water that has been contaminated by feces of an infected person [1, 2]. According to World Health Organisation, most recent estimates approximately 21 million cases and 2, 22,000 typhoid deaths were found to be reported annually throughout the world. Annually in the United States about 300-400 cases were reported and the disease is expected to occur in about 6,000 people per year. The rate of death may be as high as 25% without treatment, while with treatment it is between 1- 4% [3,4]. Definite antimicrobial therapy reduces the clinical symptoms associated with typhoid fever and reduces the risk for death. Fluoroquinolones are the empiric treatment in most parts of the world for the management of typhoid fever but unfortunately, they are contraindicated in paediatric patients and pregnant women due to its damage to the articular cartilage. However, fluoroquinolone-resistant or multidrug-resistant (MDR) (resistant to chloramphenicol, trimethoprim-sulfamethoxazole and ampicillin) strains are common in the developing countries such as India and Africa [5-7]. In the search for alternative antibiotics for the treatment of MDR typhoid fever, the third generation cephalosporins have shown good activity against *Salmonella* Typhi [8, 9].

Cefixime, oral third generation cephalosporin antibiotic was reported to be more effective in treating MDR typhoid fever particularly in children from endemic areas [10, 11]. The bactericidal action of Cefixime is due to the inhibition of cell wall synthesis by binding at penicillin binding proteins thus inhibiting peptidoglycan synthesis inside bacterial cell wall leading to bacterial cell death. The major drawback with cefixime was its poor solubility in biological fluids and thus leading to poor bioavailability (40-50%) and with a half-life of 2-3 h. Therefore, it leads to the administration of 200mg twice daily for 1-2 weeks [12]. To overcome the confines associated with current conventional dosage regimen a novel drug delivery approach is necessary.

Nanoparticle research is currently an area of intense scientific interest due to a wide variety of potential applications in biomedical, optical and electronic fields. Nano-particulate drug delivery systems has emerged as a promising novel drug delivery approach for the treatment of enteric infectious diseases by targeting and sustaining the drug release inside the targeted cells [13-15].

The polymeric nanoparticles have been broadly studied as particulate carriers in the pharmaceutical and medical fields as drug delivery vehicles due to its improved bioavailability, reduced plasma opsonisation, better encapsulation, controlled release of drug, bio-compatible with less toxic properties and improved patient compliance. Chitosan is a deacetylated form of chitin, an abundant

polysaccharide present in crustacean shells. Chitosan is a biodegradable and biocompatible cationic polymer having good mucoadhesive and membrane permeability properties [16-18]. Chitosan gained interest in nanoparticulate oral drug delivery as a vehicle because it is able to reduce the trans epithelial resistance and opening the tight junction between epithelial cells and due to its good mucoadhesive property it has been used as a carrier for sustained drug delivery. The major limitation of chitosan is restricted by its faster dissolution in stomach and its limited capacity for controlled drug release [19, 20]. To overcome the limitations associated with chitosan, poly electrolyte complexes are formed by interactions between molecules that carry oppositely charged ionisable groups [21-23]. Mucilages are promising biodegradable polymers of natural origin that are extensively used for conventional and novel dosage forms and have a variety of applications in field of pharmacy as binders, suspending agents, sustaining agent and gelling agent in novel drug delivery dosage forms [24-26].

The study was aimed to fabricate and to characterize the natural polymer based cefixime nanoparticles prepared using chitosan and *Basella alba* leaf mucilage as matrix to sustain the drug release inside the infected cells to achieve better therapeutic concentration at the targeted site with increased bioavailability and half-life.

## MATERIALS AND METHODS

### Materials

Cefixime was obtained as a gift sample from Kniss laboratories Pvt Ltd, Chennai, India. Chitosan was procured from Sigma-Aldrich Chemical Co. Ltd. All other chemicals used were of analytical grade and double distilled water was used throughout the experiments.

### Extraction and purification of *Basella alba* leaf mucilage

*Basella alba* leaves (250g) were shade dried in sunlight for ten days and powdered in a mechanical blender and soaked in distilled water (500 ml) for 24 hours in a round bottomed flask then heated at 50°C for 2h. The water soluble fraction of mucilage is extracted as per the procedure reported previously [27].

### Preparation of cefixime nanoparticles

The cefixime nanoparticles were prepared using coacervation method reported earlier with slight modification [28, 29]. The purified mucilage solution (0.04% w/v) was dissolved in distilled water and kept under magnetic stirring and pH of the solution was adjusted to 5.2 using 0.1N HCl. The chitosan (0.02% w/v) was dissolved in a solution of 0.1% v/v acetic acid was kept under magnetic stirring and pH of the solution was adjusted to 5.5 using 1N NaOH, a constant amount of cefixime 0.05% (w/v) was added to the chitosan solution with constant stirring at 3500 rpm. The mucilage solution was added slowly drop wise to the mixture of chitosan and cefixime at a different polymeric ratios to give four different formulations i.e., F1 (1:1), F2 (2:1), F3 (1:2), F4 (2:2) then centrifuged at 12000 rpm for 45 min and freeze dried. The prepared cefixime nanoparticles were stored in desiccator until further use.

### Structural characterization of *Basella alba* leaf mucilage by FT-IR, GC-MS, XRD

The FT-IR spectrum of *Basella alba* leaf mucilage was recorded using FT-IR spectrophotometer. The sample were mixed with KBr in ratio of (1:4) and pressed into pellets under mechanical pressure using hydraulic press. The scans were obtained with a spectral resolution of 2cm<sup>-1</sup> from wave number 4000 to 500 cm<sup>-1</sup> [30]. The GC-MS analysis was carried out using HP-5 conventional capillary column (30m x 0.25mm with internal diameter of 0.25µm) coupled to ion trap mass spectrometry functioned at 70ev. The columns were automated from 50 to 250 °C at 50 °C/min [31]. X-ray diffraction patterns of mucilage was carried out using Shimadzu, XRD 6000 equipment, with nickel filtered tube CuKα1 at a voltage of 45 kV and current of 45 mA, The scanned angle was set at 2θ from 10° to 90° and scanned rate was 1°/min to determine the crystallinity of the sample [32].

### Drug-polymer compatibility studies

FT-IR, XRD and proton NMR studies were carried out to determine the possible interaction between the drug and excipients used. FT-IR and XRD analysis were carried out as reported earlier. The proton NMR spectra of *Basella alba* leaf mucilage was recorded in an NMR spectroscopy (varian, UNITY-400, Switzerland). 100 mg of sample was dissolved in D<sub>2</sub>O and chemical shifts were reported in ppm relative to an internal standard TMS (tetramethylsilane) for <sup>1</sup>H NMR. The proton NMR spectrum was obtained at a base frequency of 400MHz and with 16 transitions at a delay time 2 seconds. The chemical shifts were expressed in δ (ppm) relative to the resonance of internal TMS. The existence of an interaction is detected by the alteration, shift or disappearance of a characteristic peak of the drug

### Physicochemical characterization of cefixime nanoparticles

#### Particle size, poly dispersity index (PDI) and zeta potential

Nanoparticles size distribution and zeta potential was determined using Nanoparticle analyser SZ-100. The average size distribution analysis was performed at a scattering angle of 90° and at a temperature of 25°C using samples suitably diluted with Isopropanol. PDI is a parameter used to define the particle size distribution of nanoparticles obtained from nanoparticle analyser. PDI ranges from a value of 0.01 - 0.06 as monodisperse, between 0.1 and 0.2 as narrowly distributed and between 0.25 - 0.7 as broadly distributed and value above 0.7 indicated extremely broad size distribution that cannot be described by means of PDI. The zeta potential was measured using a disposable zeta cuvette using samples appropriately diluted with double distilled water [33-35].

#### Morphology studies by Scanning electron microscopy (SEM), Transmission electron microscopy (TEM), Atomic force microscopy (AFM)

The morphology of nanoparticles was studied using a scanning electron microscope (Hitachi S 3000H, Japan). The nanoparticles were fixed to the plate surface with double-sided adhesive tape, a thin coating of gold was applied and surface features were observed. TEM was used to study the surface morphology of nanoparticles. 5 µl of

nanoparticles suspension were dropped onto formvar-coated copper grids and dried in hot air oven for 45 min then the samples were stained using 2% w/v phosphotungstic acid. Digital Micrograph and soft imaging viewer software were used to perform the image capture [36]. AFM was performed to confirm the surface morphology by dissolving the nanoparticles appropriately in Isopropyl alcohol was placed on a glass slide and dried overnight to form a thin film and was analysed by AFM(NT-MDT).

#### Determination of % Entrapment efficiency and % drug content

The amount of drug entrapped in nanoparticles was determined from the clear supernatant obtained after centrifugation of nanoparticles at 12,000 rpm at 5 °C for 45 min and determined by UV-Vis spectrophotometer at 287 nm [37-39]

$$\% \text{ Entrapment efficiency} = \frac{(\text{Actual drug content}) \times 100}{(\text{Theoretical drug content})}$$

$$\% \text{ Drug content} = \frac{(\text{Weight of drug in nanoparticles}) \times 100}{(\text{Weight of nanoparticles})}$$

#### In-vitro drug release by diffusion bag technique

In-vitro drug release studies for the nanoparticles were performed using diffusion bag technique. The cefixime nanoparticles (equivalent to 20mg) dispersed in 5ml of dissolution medium was placed in a dialysis bag immersed in USP Apparatus I in 300 ml of 0.05 M potassium phosphate buffer pH 7.4 stirred at 37 ±1°C at 100 rpm. Aliquots of 1 ml were withdrawn at regular intervals of time and an equal volume of buffer solution was added to maintain the constant volume of dissolution fluid. The percentage drug release was measured spectrophotometrically by UV at 287nm [40-42]. The results obtained from in-vitro drug release studies were fitted into various kinetic models such as Zero order release kinetics, First order release kinetics, Higuchi classical diffusion equation, Koresmeyer-Peppas's exponential equation and Hixson-Crowell erosion equation to know the mechanism of drug release. The equation with high regression coefficient ( $r^2$ ) for formulation will be the best fit of release data. For Koresmeyer-Peppas's equation,  $n = 0.5$  indicates pure fickian diffusion,  $n = 0.5-1$  indicates anomalous non-fickian diffusion and  $n=1$  indicates zero order release [43, 44].

#### In-vitro antimicrobial efficiency by disc agar diffusion technique and broth dilution technique

The antibiotic-resistant profile of sample was determined by disc diffusion method to determine the zone of inhibition. The study was carried out on Muller Hinton agar (MHA) medium. Then the inoculums were spread on to the solid plates with sterile swab moistened with the bacterial suspension (*Salmonella Typhi*). 20 µl of pure drug (cefixime) and cefixime nanoparticles were serially diluted to a different concentration of 62.5 µg/ml, 125 µg/ml, 250 µg/ml, 500 µg/ml and 1000 µg/ml was added to respective disc placed on MHA plates. These plates were incubated for 24 h at 37 °C. Then the activity was determined by measuring the diameter of zone of inhibition [45]. The MIC50 of pure drug and formulation was determined using broth dilution technique by adding 5 ml of sterilized

nutrient broth in each tube. To this 100 µl of bacterial culture (*Salmonella Typhi*) was added and then 100 µl of different concentration of samples (62.5 µg/ml, 125 µg/ml, 250 µg/ml, 500 µg/ml and 1000 µg/ml) was added. OD was measured at 620 nm [46].

## RESULT AND DISCUSSION

### Characterization of mucilage by FT-IR, GC-MS and XRD

From the FT-IR spectra of *Basella alba* leaf mucilage mucilage at 3419.90  $\text{cm}^{-1}$  indicates OH stretching of hydroxyl group, the characteristic peak at 2923.96  $\text{cm}^{-1}$  corresponds to C-H stretching band of carboxyl group, the absorption band at 2145.26  $\text{cm}^{-1}$  corresponds to C=C stretching band, the peak at 1627.01  $\text{cm}^{-1}$  represents stretching mode of keto groups, the band at 1426.45  $\text{cm}^{-1}$  represents C-H bending mode, the peak at 1107.42  $\text{cm}^{-1}$  suggest the presence of stretching vibrations of C-OH group, the frequency at 621.77  $\text{cm}^{-1}$  indicates rocking vibrations of C-H group (Figure 1). This findings has been supported in other studies reported earlier [12]. The GC-MS analysis of hydrolysed fraction of *Basella alba* leaf mucilage showed four peaks at retention time (RT) of 10.65 min, 8.75 min, 7.41 min, 6.61 min, 5.93 min, 5.32 min with molecular ion peaks of m/z ratio, 317.5, 194.67, 179.62, 146.83, 150.10, 146.81 respectively indicating the presence of D-arabinose, D-galacturonic acid, xylose and rhamnose (Figure 2). From XRD studies no characteristic peaks were observed which indicates that the mucilage was found to be amorphous in nature (Figure 3)

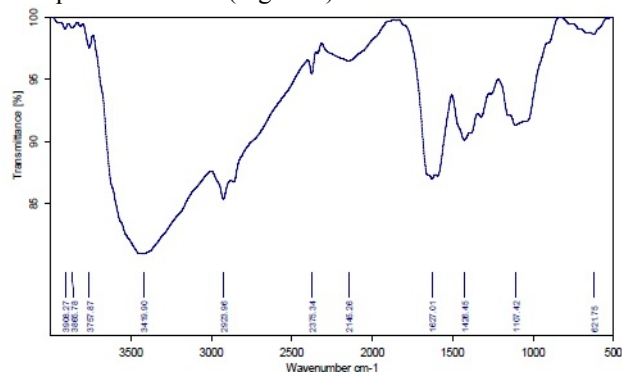


Figure 1: FT-IR spectra of *Basella alba* leaf mucilage at a resolution of 2 $\text{cm}^{-1}$  from 4000 to 500 $\text{cm}^{-1}$

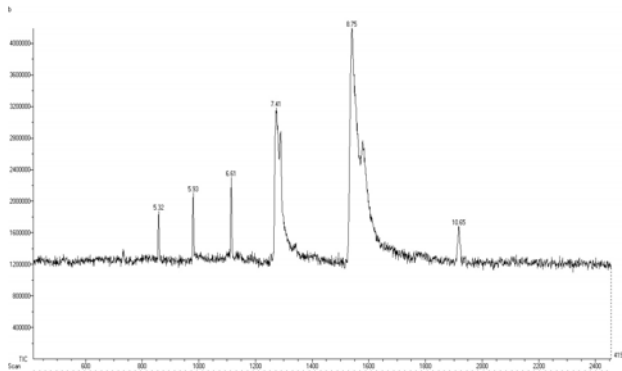
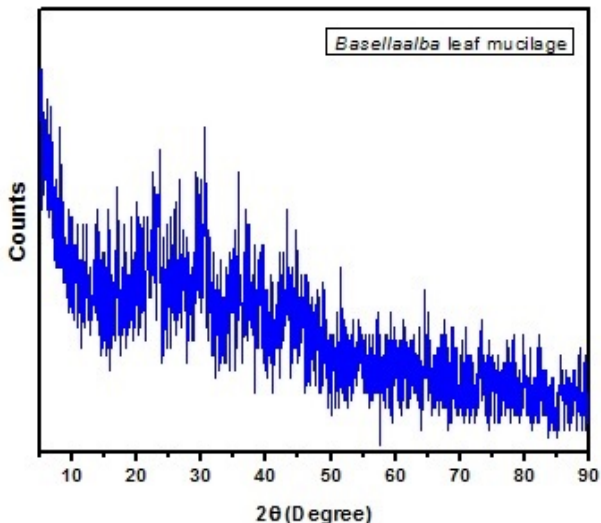


Figure 2: GC-MS of hydrolyzed fraction of *Basella alba* leaf mucilage showing peaks at retention time indicating the presence of major sugars and uronic acid



**Figure 3:** X-ray diffraction pattern of *Basella alba* leaf mucilage scanned at an angle  $2\theta$  from  $10^\circ$  to  $90^\circ$  and scanned rate was  $1^\circ/\text{min}$ .

**Drug-polymer compatibility studies by FT-IR, proton NMR and XRD spectroscopy**

The FT-IR spectra of cefixime, *Basella alba* leaf mucilage, chitosan and its physical mixture containing drug were analysed. There were no changes in the peak shape and no shift of peaks of drug in the physical mixture containing drug and polymer. Hence there is no chemical interaction between drug and polymers used (Figure 4). The proton NMR spectra of cefixime and its physical mixture with polymers were analysed. The presence of characteristic peak of drug in the physical mixture indicates that there were no changes in the proton assignments of drug (Figure 5). Hence there is no incompatibility between drug and polymers used. The X-ray diffraction pattern of drug and the formulation were carried out. The pure drug confers crystalline nature with sharp peak between  $7.96^\circ 2\theta$  to  $26.37^\circ 2\theta$  a characteristic of cefixime that represent the crystalline nature of the drug, the same diffraction was also observed in the prepared formulation with decreased intensity of signal indicating no signs of incompatibility between the pure drug and formulation components (Figure 6).

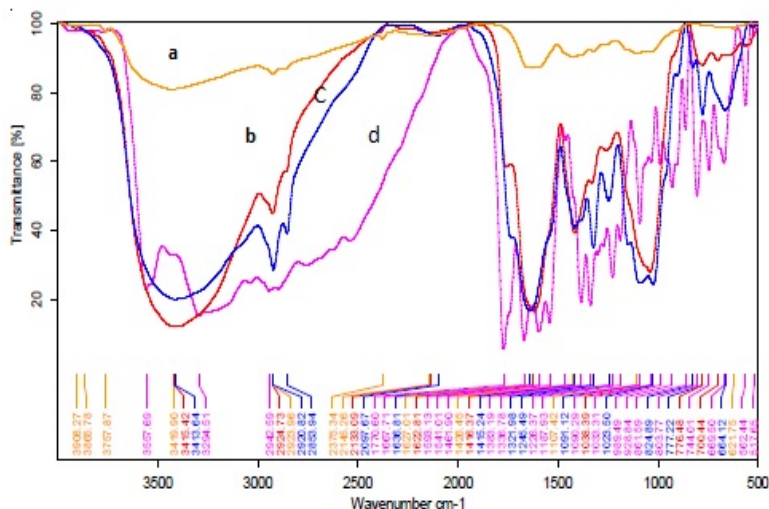


**Figure 4:** FT-IR spectra of a) *Basella alba* leaf mucilage b) Chitosan c) Cefixime d) Physical mixture containing drug and polymers

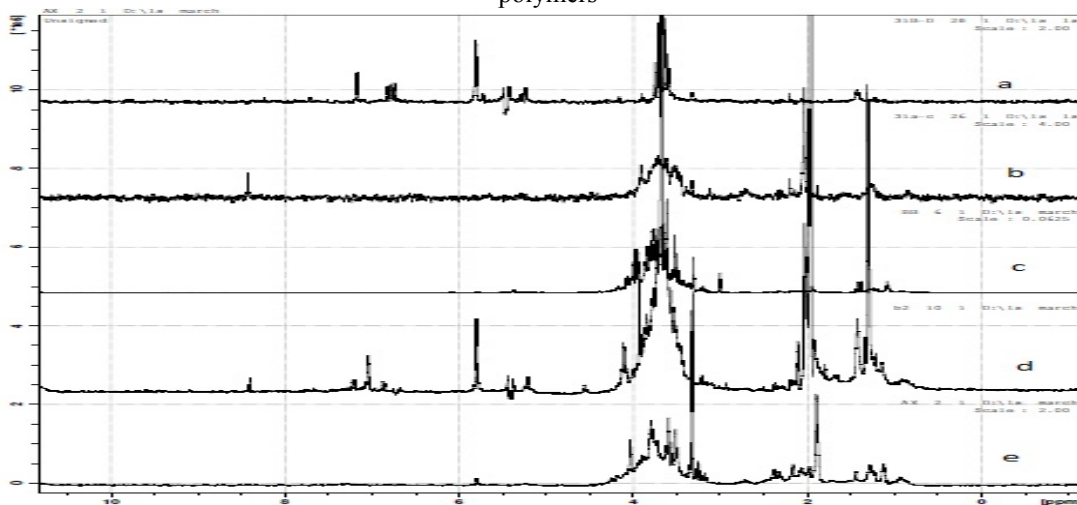


**Figure 5:** Proton NMR spectra of a) Cefixime b) Chitosan c) Placebo d) Physical mixture containing drug and polymers e) *Basella alba* leaf mucilage

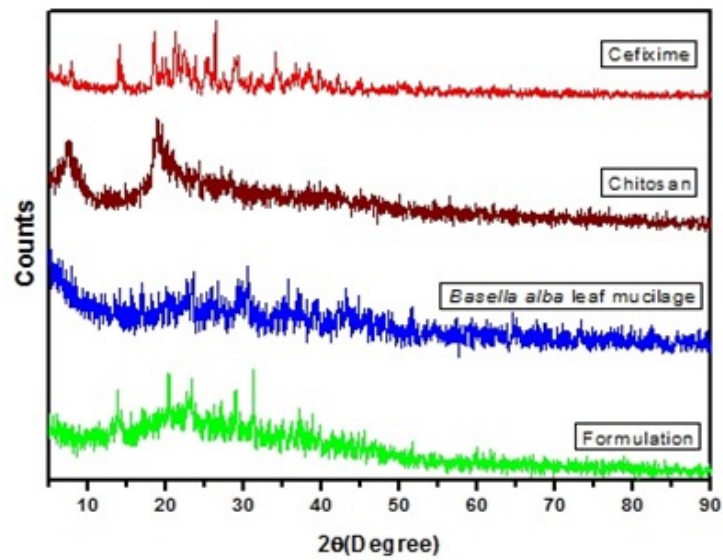


**Figure 6:** XRD pattern of Cefixime, Chitosan, *Basella alba* leaf mucilage and Formulation

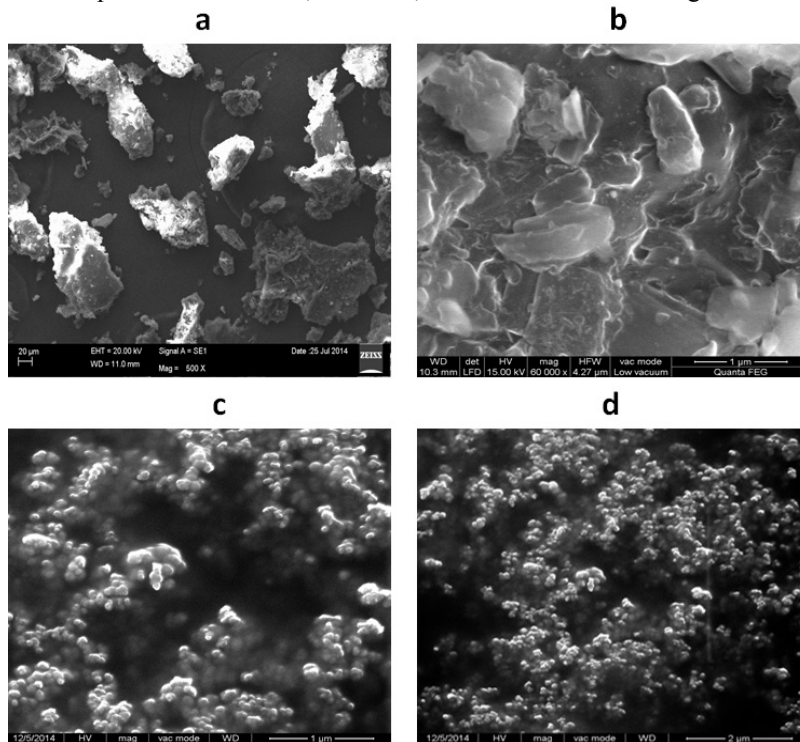


**Figure 7:** FE-SEM image of a) *Basella alba* leaf mucilage b) chitosan c) cefixime nanoparticles at higher magnification d) cefixime nanoparticles at lower magnification

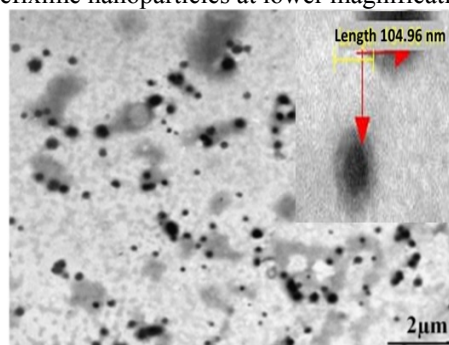


**Figure 8:** TEM morphology of cefixime nanoparticles representing spherical shape, smooth surface, solid dense structure with a particle size ranging between 100 nm - 350 nm

**Table 1: Characterization of prepared cefixime nanoparticles \***

Formulation	Average Size mean (nm)	Poly dispersity index	Zeta potential (mV)	%Entrapment efficiency	%Drug content
F1	165.6±6.5	0.211	13.1	72.6±3.1	80.8±1.5
F2	194.6±9.6	0.324	-38.3	80.5±4.5	82.2±0.4
F3	265.0±11.2	0.452	66.4	77.3±2.9	78.9±1.0
F4	399.8±6.3	0.752	14.3	71.6±1.2	65.2±2.2

\* Data represented as mean± SD, n=3.

#### Determination of particle size, poly dispersity index (PDI), zeta potential, % entrapment efficiency and % drug content of the cefixime nanoparticles

The average particle size and PDI was found to be increase with polymer concentration. The Formulations F2 and F3 with Zeta Potential < -30 mV and > +30mV respectively, shows high degrees of stability with no aggregation. In addition, from the zeta potential measurement, the dominated component on the particles surface for formulation F2 was predicted as mucilage, being negatively charged polymer imparts anionic nature to nanoparticles, whereas for F3 the dominated component on the particles surface was predicted as chitosan which imparts cationic nature to the nanoparticle. The zeta potential value for F1 and F4 formulations was found to be approximately neutral. The % entrapment efficiency and % drug content was found to be increased with increase in polymer concentration, but in formulation F4 due to increase in size the surface area of nanoparticles was decreased which leads to the decreased drug entrapment efficiency and drug content as shown in Table 1.

#### Morphological studies of prepared nanoparticles were carried out using Scanning Electron Microscopy (SEM), Transmission Electron Microscopy (TEM) and Atomic Force Microscopy (AFM)

The SEM studies revealed that the surface morphology of the prepared formulation was found to be spherical, smooth surface with solid dense structure (Figure 7). The TEM images indicate that the nanoparticles with spherical shape in size range between 100 nm to 350 nm (Figure 8). The AFM studies revealed the three-dimensional view of the nanoparticles as spherical and discrete with average particle size of 160 nm (Figure 9). The nanoparticles appeared to be in same diameter with SEM, TEM and AFM as compared

to average particle size measured using nanoparticle analyser.

#### *In-vitro* drug release studies by diffusion bag technique

From *in-vitro* drug release study by bag diffusion technique showed a biphasic pattern with initial burst release followed by sustained release of drug up to 24h. The F2 showed sustained drug release of 99.53% at the end of 24h compared to other formulations. The amount of drug release was decreased with increase in polymer concentration due to increase in the thickness of the polymeric membrane which decreases the diffusion of drug through it (Figure 10). The data obtained from drug release study were extrapolated by Zero order, First order, Higuchi matrix, Hixson-Crowell, Korsmeyer Peppas's equations to know the mechanism of drug release from these formulations. Based on the highest regression coefficient value ( $r^2$ ) the best fit model for all formulations was found to be Higuchi model ( $r^2$ : 0.97-0.98). The release of drug from the polymer matrix containing hydrophilic polymers involves diffusion. To confirm the diffusion mechanism the data was fitted into Koresmeyer-Peppas's equation, based on 'n' values ranging from 0.5-1 the drug release was found to follow anomalous non-fickian diffusion i.e. the increased diffusivity of drug from the matrix by solvent-induced relaxation of the polymers (Figure 11).

#### *In-vitro* antimicrobial efficiency

The DAD technique revealed that pure drug yielded 9 mm clear zone surrounding the disc whereas prepared formulation discs produced 13 mm clear zone at a concentration of 125 µg/ml (Figure 12). The MIC<sub>50</sub> values from broth dilution technique for the pure drug and prepared formulation for *Salmonella* Typhi isolates was found to be 250 µg/ml (Figure 13)

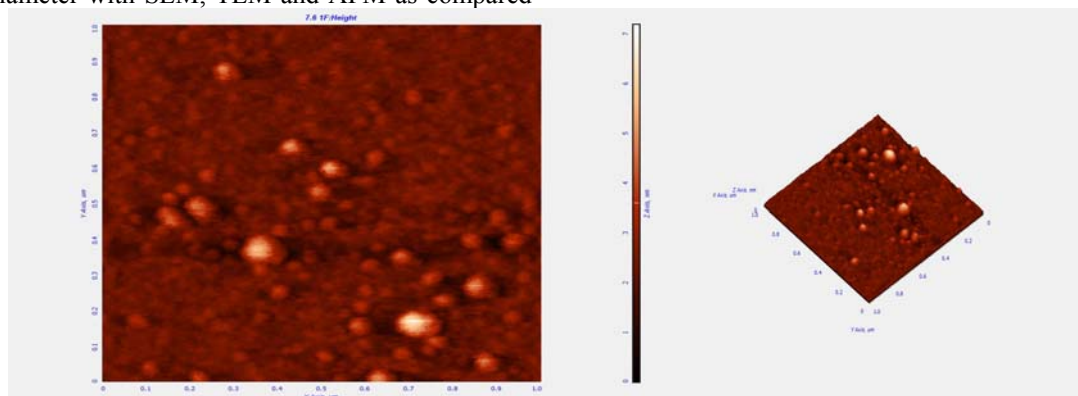


**Figure 9:** AFM image Left: cefixime nanoparticles scanned with the AFM (NT-MDT). Mean  $\sigma$  of nanoparticles is 160 nm. Scan size is 1µm x 1µm. Right: 3D view of 1µm x 1µm scan of calibrated nanoparticles

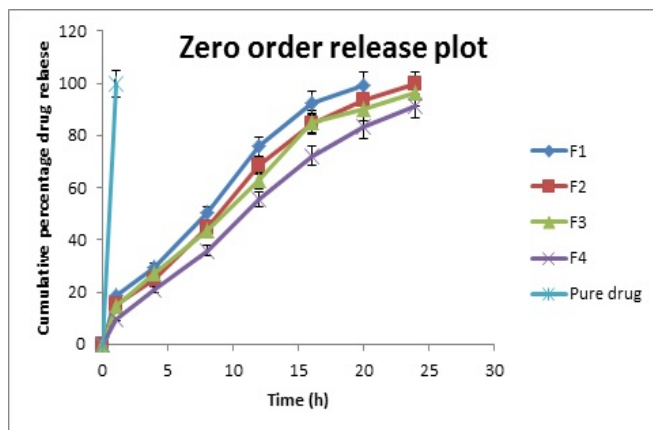


**Figure 10:** *In-vitro* drug release profile of prepared formulations in PBS (pH 7.4) at 37°C

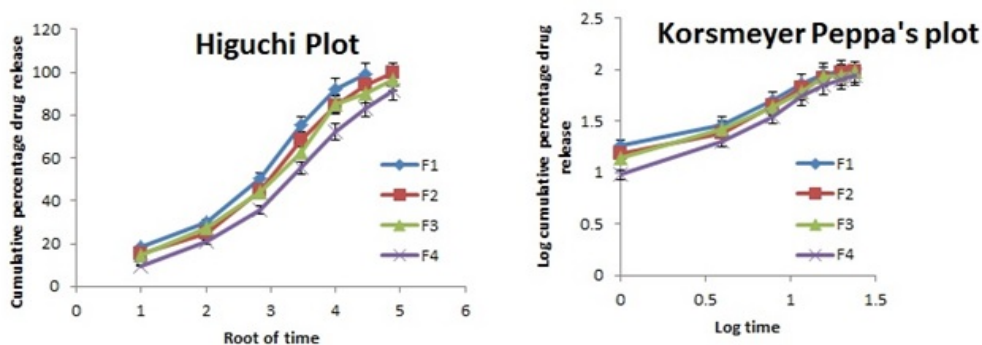


**Figure 11:** Curve fitting data analysis of all the formulations by Higuchi's plot and Koresmeyer-Peppas's plot

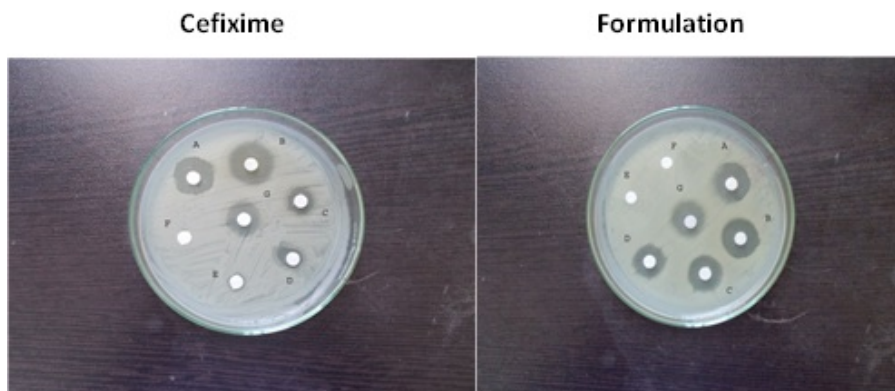


**Figure 12:** Determination of zone of inhibition (mm) by disc agar diffusion technique of the selected formulation (F2) at different concentrations. A. 1000 µg/ml B. 500 µg/ml C. 250 µg/ml D. 125 µg/ml E. Blank F. DMSO (Negative control) G. Streptomycin (10µg/ml) to respective disc.

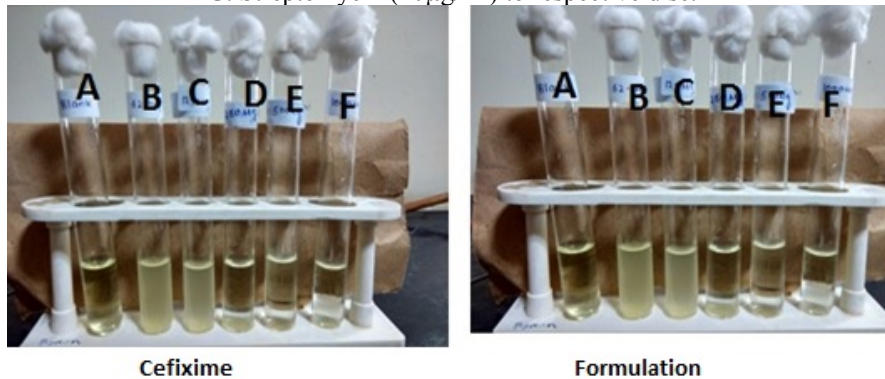


**Figure 13:** Determination of MIC by broth dilution technique of the selected batch (F2) at different concentration. A. DMSO (Negative control) B. 62.5 µg/ml C. 125 µg/ml D. 250 µg/ml E. 500 µg/ml F. 1000 µg/ml.

### CONCLUSION

The developed natural based cefixime nanoparticles showed sustained drug release compared to pure drug suspension with enhanced *in-vitro* antimicrobial efficiency with better zone of inhibition thereby achieving better therapeutic efficacy with better patient compliance followed by the declining the limitations associated with conventional dosage form.

### ACKNOWLEDGEMENT

The authors were grateful for the financial support from DST-SERB (Government of India) to carry out the above research. We sincerely acknowledge DST-PURSE centre, S.V.University for providing facility for nanoparticle size analyser and AFM facility for analysis. The authors also acknowledge IIT, Madras for providing facility for GC-MS analysis, Madras Veterinary College for providing facility for TEM analysis.

### REFERENCES

- [1] Crump, J.A., Mintz, E.D., *Clin Infect Dis.* 2010, *50*, 241–246.
- [2] Wain, J., Hendriksen, R.S., Mikoleit, M.L., Keddy, K.H., Ochiai, R.L., *Lancet.* 2015, *385*, 1136–1145.
- [3] Wallace, MR., Yousif, A.A., Mahroos, G.A., Mapes, T., Threlfall, E.J., Rowe, B., Hyams, K.C., *Eur J Clin Microbiol Infect Dis.* 1993, *12*, 907–910.
- [4] Gupta, S.K., Medalla, F., Omondi, M.W., Whichard, J.M., Fields, P.I., Gerner-Smidt, P., *Clin Infect Dis.* 2008, *46*, 1656–1663.
- [5] Snyder, M.J., Perroni, J., Gonzalez, O., Palomino, C., Gonzalez, C., Music, S., DuPont, H.L., Hornick, R.B., Woodward, T.E., *J Infect Dis.* 1973, *128*, 734–737.
- [6] Calderon, E., *J Infect Dis.* 1974, *129*, 219–221.
- [7] Soe, G.B., Overturf, G.D., *Rev Infect Dis.* 1987, *9*, 719–736.
- [8] Wallace, M.R., Yousif, A.A., Mahroos, G.A., Mapes, T., Threlfall, E.J., Rowe, B., Hyams, K.C., *Eur J Clin Microbiol Infect Dis.* 1993, *12*, 907–910.
- [9] Counts, G.W., Baugher, L.K., Ulness, B.K., Hamilton, D.J., *Eur J Clin Microbiol Infect Dis.* 1988, *7*, 428–431.
- [10] Roberto, M.S., Gerardo, R.G., Ismael, H.B., Eduardo, M.G., *Proc. West Pharmacol. Soc.* 2000, *43*, 65–66.
- [11] Memon, I.A., Billoo, A.G., Memon, H.I., *South Med J.* 1997, *90*, 1204–1207.
- [12] Muruges, S., Badal, K.M., *Trop J Pharm Res.* 2013, *12*, 155–161.
- [13] Ping, L.i., Dai, Y.N., Zhang, J.P., Wang, A.Q., *Int J Biomed Sci.* 2008, *4*, 221–228.
- [14] Jie, S., Diane, J. B., *Drug Deliv Transl Res.* 2013, *3*, 409–415.
- [15] Chan, J.M., Valencia, P.M., Zhang, L., Langer R, Farokhzad, O.C., *Methods Mol Biol.* 2010, *624*, 163–75
- [16] Adlin, J., Anton Smith, A., *Asian J Pharm Sci.* 2012, *7*, 80–84.
- [17] Muruges, S., Badal, K.M., *Trop J Pharm Res.* 2013, *12*, 155–161.
- [18] Avadi, M.R., Sadeghi, A., Mohammadpour, N., Abedin, S., Atyabi, F., Dinarvand, R., Tehrani, M., *Nanomedicine.* 2010, *6*, 58–63.
- [19] Varshosaz, J., Tavakoli, N., Moghaddam, F., Ghassami, E., *Farmacia.* 2015, *63*, 65–73.
- [20] Shely, S., Ahuja, M., Ashok, K., *Int J Biol Macromol.* 2013, *61*, 411–415.
- [21] Naidu, V.G.M., Madhusudhana, K., Sashidhar, R.B., Ramakrishna, S., Roop, K.K., *Carbohydr Polym.* 2009, *76*, 464–471.
- [22] Haroldo, C.B., Fernanda, F.M., Flavia, O.M.S., Regina, C.M., *J Braz Chem Soc.* 2010, *21*, 2359–2366.
- [23] Shanmuganathan, S., Shanmugasundaram, N., Adhirajan, N., Ramyaalakshmi, T.S., Marybabu, S., *Carbohydr Polym.* 2008, *73*, 201–211.
- [24] Nagavarma, B. V. N., Hemant, K.S., Ayaz, A., Vasudha, L.S., Shivakumar, H.G., *Asian J Pharm Clin Res.* 2012, *5*, 16–23.
- [25] Aggarwal, S., Goel, A., Sandeep, S., *Adv. Polym. Sci.* 2012, *2*, 1–15.
- [26] Clochard, M., Dinand, E., Rankin, S., Simic, S., Brocchini, S., *J Pharm Pharmacol.* 2001, *53*, 1175–1184.
- [27] Vijender, P., Manjit, S., Bhat, Z. A., Popinder, S., Dinesh, K., Sheela, S., *J Pharm Res.* 2010, *3*, 1892–1894.
- [28] Douglas, K.L., Tabrizian, M.J., *J Biomater Sci Polym Edn.* 2005, *16*, 43–56.
- [29] Gomathi, T., Govindarajan, C., Maximas, H.R., Sudha, P.N., Mohamed Imran, P.K., Venketesan, J., Kim, S., *Int. J. Pharm.* 2014, *468*, 214–222.
- [30] Shanmuganathan, S., Harika, B., Abdul Ahad, H., *Int. J. Pharm. Sci. Rev. Res.* 2014, *24*, 115–119.
- [31] Deepa, P., Prashant, K., Gowthamarajan, K., Ankur, G., Bhagyashree, K., Ashish, W., *Nanotoxicology.* 2014, *8*, 843–855.
- [32] Hemanta Kumar, S., Sunita, L., Lila, K., *Acta pharm.* 2013, *63*, 209–222.
- [33] Xu, Q., Crossley, A., Czernuszka, J., *J. Pharm. Sci.* 2009, *98*, 2377–2389.
- [34] Sengel-Turk, C.T., Hascicek, C., Dogan, A.L., Esendagli, G., Guc, D., Gonul, N., *Drug Dev. Ind. Pharm.* 2012, *38*, 1107–1116.
- [35] Yong, Li., Xiuhua, Z., Yuangang, Z., Yin, Z., *Int. J. Pharm.* 2015, *490*, 324–333.
- [36] Marisa, C., Joao, J.S., Alberto, A.C.C., Olga, C., Dina, M., Elisa, S., Frederic, T., Jean-Christophe, O., *Eur J Pharm Biopharm.* 2015, *96*, 65–75
- [37] Avadi, M.R., Sadeghi, A.M.M., Dounighi, N.M., Abedin, S., Atyabi, F., Dinarvand, R., Rafiee-Tehrani, M., *Nanomed Nanotechnol.* 2010, *6*, 58–63.
- [38] Sanna, V., Rogio, A.M., Siliani, S., Piccinini, M., Marceddu, S., Mariani, A., Sechi, M., *Int J Nanomedicine.* 2012, *7*, 5501–5516.
- [39] Bendas, E.R., Abdelbary, A.A., *Int. J. Pharm.* 2014, *468*, 97–104.
- [40] Sanjay, K.M., Shruti, C., Sushma, T., Kanchan, K., Farhan, J.A., Roop, K.K., *Eur J Pharm Biopharm.* 2008, *68*, 513–525.
- [41] Evans, D.F., Pye, G.E., Bramley, R., Clark, A.G., Dyson, T.J., Hardcastle, J.D., *Gut.* 1988, *29*, 1035–41.
- [42] Akansha, T., Ranjana, G., Shubhini, A., *Int J PharmTech Res.* 2010, *2*, 2116–2123.
- [43] Siepmann, J., Siepmann, F., *Int. J. Pharm.* 2011, *418*, 42–53.
- [44] Sackett, C.K., Narasimahan, B., *Int. J. Pharm.* 2011, *418*, 104–114.
- [45] Subhankari Prasad, C., Sumanta Kumar, S., Panchanan, P., Somenath, R., *Asian Pac J Trop Biomed.* 2012, *2*, 215–219.
- [46] Koopai, M.N., Maghazei, M.S., Mostafavi, S.H., Jamalifar, H., Samadi, N., Amini, M., Malek, S.J., Darvishi, B., Atyabi, F., Dinarvand, R., *DARU J Pharm Sci.* 2012, *20*, 1–8.